Mihailo TRIFUNAC

DESIGN OF STRUCTURES CROSSING ACTIVE EARTHQUAKE FAULTS

Mihailo D. Trifunac
Department of Civil Engineering, University of Southern California,
Los Angeles, California, 90089-2531

Summary
The classical response spectrum method (RSM) was developed in 1932 for excitation by synchronous ground motion at all supports. It is shown in this paper how RSM can be generalized to the analyses of extended structures, (1) experiencing differential in-plane, and out-of-plane ground motions, and (2) crossing active faults. A relative displacement spectrum for design of bridge columns, or of first-story columns in buildings, SDC (T, T_T, ζ, ζ_T, τ), is defined. In addition to the natural periods of the in-plane response, T_{IN}, and of the out-of-plane response, T_{OP}, such that $T_{IP} \sim T_{OP} \sim T$, and the corresponding fractions of critical damping, $\varsigma_{IP} \sim \varsigma_{OP} \sim \varsigma$, this spectrum also depends on the fundamental period of torsional vibrations, T_T, and the corresponding fraction of critical damping, ζ_T, on the "travel time," τ (of the waves in the soil over a distance of about one-half the length of the building, or the distance, L, between the bridge columns), and on the fault dislocation amplitudes. The new spectrum, SDC, can be estimated by using the empirical scaling equations for (1) relative displacement spectra, SD, (2) for peak ground velocity, v_{max}, and (3) empirical equations for prediction of fault slip in terms of fault dimensions and earthquake magnitude. Computation of the new SDC spectra is illustrated for a hypothetical fault and a long continuous bridge, with a rigid superstructure.
Key words: Differential ground motion, response spectra, earthquake fault displacement

1. Introduction

The common use of the classical response spectrum method, for design of earthquake resistant structures, assumes that all points of building foundations move synchronously and with the same amplitudes. This, in effect, implies that the wave propagation and permanent deformation in the soil can be neglected. Unless the structure is long (e.g., a bridge with long spans, a dam, a tunnel) or "stiff" relative to the underlying soil, these simplifications are justified and can lead to a selection of approximate design forces. Approximate analyses suggest that when $a/\lambda < 10^{-4}$, where a is wave amplitude of ground motion and λ is the *corresponding* wavelength, the wave propagation effects on the response of simple structures can be neglected (Todorovska and Trifunac, 1990).

The purpose of this paper is to show how the response spectrum method can be extended for the design of long structures, with multiple supports (e.g., bridges), when those have to cross an active fault. For this it is necessary to combine the simultaneous action of: (1) the dynamic forces caused by shaking, (2) the differential motions resulting from wave passage, and (3) the permanent displacements of the foundations caused by faulting.

2. Static and dynamic loads

Response Spectra

The dynamic response of structures, to strong ground shaking, can be characterized by the response spectrum amplitudes. Response Spectra show the maximum relative displacement, $SD(T,\varsigma)$, relative velocity ($\sim \omega SD(T,\varsigma)$), or absolute acceleration ($\sim \omega^2 SD(T,\varsigma)$) of an equivalent single degree of freedom system excited by ground shaking, where T is natural period of the oscillator, $\omega = 2\pi/T$, and ς fraction of its critical damping.

The concept of response spectrum was introduced by Biot in 1932 (Biot, 1932; 1941; 1942; Trifunac, 2006a,b) and at present it

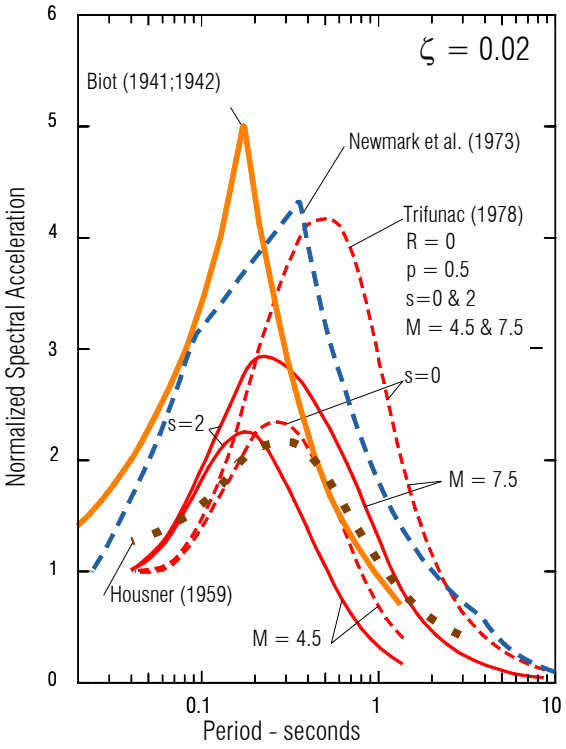

Fig. 1. Examples of four pseudo acceleration spectral shapes.

continues to be the principal tool in Earthquake Engineering for the design of structures to withstand earthquake shaking. Figure 1 illustrates four classical shapes of acceleration spectra ($\omega^2 SD(T,\varsigma)$) normalized to unit ground acceleration. The spectra of Biot (1941,1942), Housner (1959) and Newmark et al. (1973) illustrate the early attempts to define the fixed shape spectra, all scaled by one amplitude factor, usually peak design (ground) acceleration. The spectra of Trifunac (1978) illustrate the variable shape spectra. In Fig. 1 the dependence of the latter spectral amplitudes is illustrated for two different magnitudes 4.5 and 7.5, and for two site conditions: s=0 for sites on sediments, and s=2 for sites on the basement rock. Division of the spectral amplitudes in Fig. 1 by $\omega^2 = (2\pi/T)^2$ will result in the corresponding shapes of the relative displacement spectra $SD(T,\varsigma)$. Further details on empirical scaling of spectral amplitudes can be found in a review paper by Lee (2002).

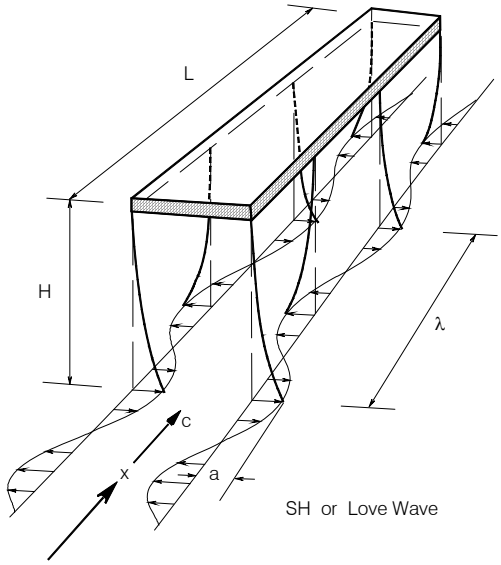

Fig.2(a) A structure excited by passage of SH or a Love Wave.

Pseudo-Static Differential Motions Caused by Wave Passage

Figures 2a and b illustrate "short" waves propagating along the longitudinal axis of a building or a multiple-span bridge. For simplicity, the incident wave motion has been separated into out-of-plane (OP) motion (Fig. 2a) and in-plane (IP) motion (Fig. 2b). The in-plane ground motion can be separated into horizontal (longitudinal), vertical, and rocking and torsional components, while the out-of-plane ground motion consists of horizontal motion in the transverse direction rocking about the longitudinal and transverse bridge axes, and torsion along the vertical axis. Trifunac and Todorovska (1997) analyzed the effects of the horizontal in-plane components of differential motion for buildings with models that are analogous to the sketch in Fig. 2b, and showed how the response spectrum method could be modified to include the first-order effects of differential motions. Trifunac and Gicev (2006) extended this approach to out of plane response of structures. Trifunac and Todorovska (1997) have shown that the relative displacement of different foundations for in-plane response to horizontal ground motion can be estimated in terms of $v_{\max}\tau$, where $v_{\max}$ is the peak ground velocity, from

$$SDC(T,\zeta,\tau) \approx \left\{u_{\max}^2 + (v_{\max}\tau)^2\right\}^{1/2} \quad . \qquad (1)$$

Likewise, Trifunac and Gicev (2006) have shown that the relative displacement of different foundations for out-of-plane response can be estimated from

$$SDC(T,T_T,\zeta,\zeta_T,\tau) \approx \left\{u_{\max}^2 + 2\left(v_{\max}\tau\right)^2\right\}^{1/2} \quad (2)$$

where T_T and ζ_T are the first natural period of the system in torsion, and fraction of the corresponding damping respectively. In Eqs. (1) and (2) SDC represents Relative Displacement Response Spectra for design of columns, and

$$\tau_i \equiv \frac{sx_i}{\beta_{av}} \ . \quad (3)$$

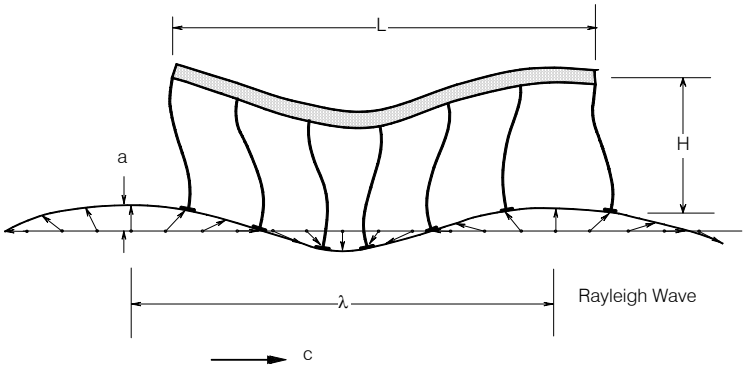

Fig. 2(b) A structure excited by passage of Rayleigh wave.

β_{av} is the average shear-wave velocity in the top 30 meters of soil, s is an empirical scaling factor that is of the order of one (Trifunac and Gicev, 2006), and x_i is the distance from a central point in the structure (or a bridge) to the i-th column being analyzed. Typical values of τ are less than 0.1 (Trifunac, 1997).

In Eq. (1) and (2) $u_{\max}$ are the relative displacement spectra $SD(T,\varsigma)$, for in-plane and out-of-plane relative displacement responses respectively, that can be estimated by dividing the spectral shapes in Fig. 1 by ω^2, or directly using empirical scaling equations (Lee, 2002; Trifunac, 1978; Lee and Trifunac, 1995a,b). For simplicity in this note, and without loss of generality, it is assumed that $T_{IP} \sim T_{OP} \sim T$, and $\varsigma_{IP} \sim \varsigma_{OP} \sim \varsigma$.

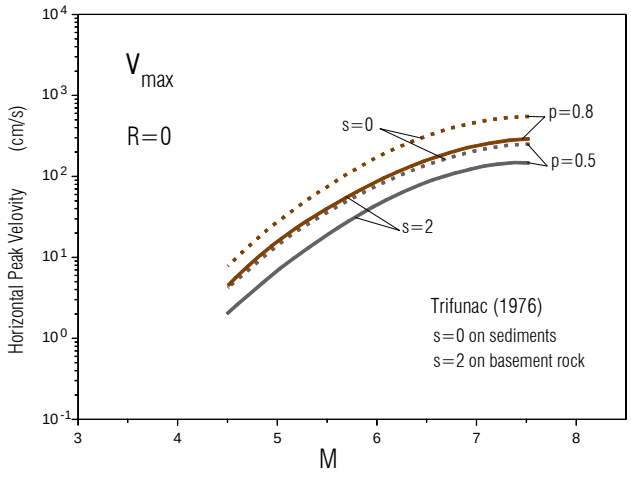

Fig. 3 Peak velocities at fault surface for two probabilities of being exceeded p = 0.5 and 0.8.

Once SDC has been evaluated, the maximum shear in the i-th column becomes

$$V_{i_{\max}} \approx k_i SDC \quad (4)$$

where k_i is the stiffness of that column.

To apply Eqs. (1) and (2) it is also necessary to have estimates of peak ground velocity at zero distance from the fault (epicentral distance R=0).
Figure 3 presents such estimates for sites on sediments (s=0) and basement rock (s=2), for probabilities of excedance p = 0.5 and 0.8, and for earthquake magnitudes between 4.5 and 7.5 (Trifunac, 1976).

Pseudo-Static Differential Motions Caused by Faulting

In densely populated areas near the continental margins, characterized by numerous faults with moderate to high seismic activity, lifelines (highway bridges and tunnels, aqueducts, gas lines) crossing active faults are not uncommon. For the design and retrofit of such structures, and for the assessment of their seismic performance, it is necessary to have rational estimates of the effects permanent ground displacement caused by seismic slip, will have on these structures. In this paper we present a *deterministic* methodology for the assessment of permanent deformation of structures crossing a fault, due to slip on that fault caused by an earthquake.

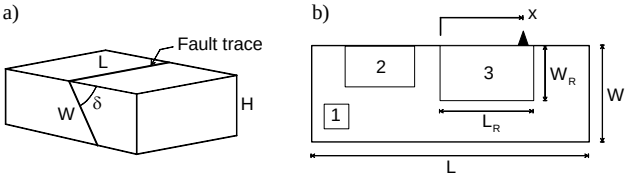

Fig. 4 The fault model.

The methodology for estimating the design criteria to account for the fault displacement involves only one fault zone. However, not every earthquake in that source zone affects the site (while every earthquake will cause some level of shaking, depending on the distance). Part (a) of Fig. 4 shows a fault with length L and width W,

dipping at angle δ, and extending from the ground surface to depth $H = W \sin\delta$. Part (b) shows the fault surface, the site by a solid triangle, and three hypothetical ruptures, one of which affects the site, another one that occurs at depth and does not break the ground surface, and a third one that breaks the ground surface, but does not extend horizontally to the site. The possible ruptures have lengths $L_R(M)$ and widths $W_R(M)$, which both depend on magnitude. Simplifying assumptions in the model are (1) that the distribution of relative displacements at the ground surface can be described by a parabola along the ruptured segment of the fault trace, with zero amplitudes at the fault ends, and maximum in the middle, and (2) that the static displacement field does not decrease with distance from the fault. This is appropriate for typical bridges, with the spans of the order of hundreds of meters, in which case this "attenuation" effect is small compared to the overall uncertainty of the estimation.

For estimating L_R and W_R one can use Trifunac (1993a,b), or Wells and Coppersmith (1994), or

$$\log_{10} L_R(M) = 0.511M - 1.934;$$
$$\log_{10} W_R = 0.229M - 0.513 \qquad (5)$$

that is derived by least squares fit through a subset of the data gathered by Wells and Coppersmith (1994) that corresponds to California earthquakes (Todorovska et al. 2005).

Fig. 5 shows L_R and W_R versus magnitude for

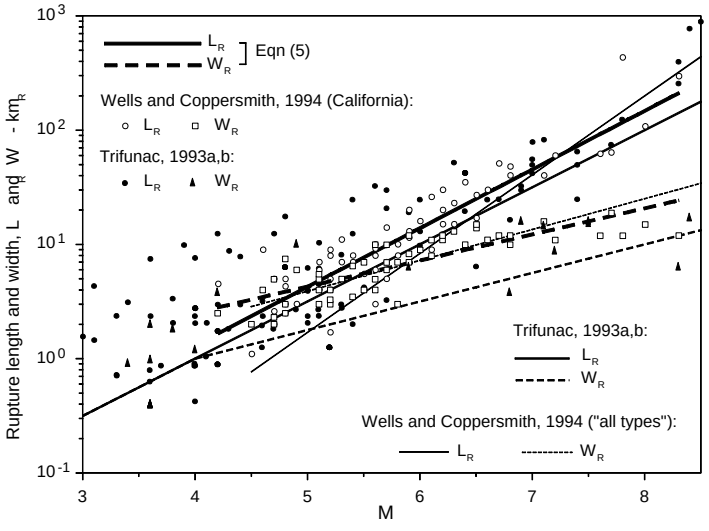

Fig. 5 Rupture length and width.

model 3 of Trifunac (1993a,b) (the medium thick lines), consistent with *seismological* estimates of rupture length and width, with theoretical earthquake source models, and with empirical scaling models of peaks and spectra of strong ground motion (Lee et al., 1995; Trifunac, 1993a). Fig. 5 also shows empirical relations for L_R and W_R of Wells and Coppersmith (1994) (the thin lines) for "all" types of faulting, derived from worldwide data, and valid for $4.8 \le M \le 7.9$. The open circles and rectangles show a subset of the data for L_R and W_R gathered by Wells and Coppersmith (1994) for earthquakes in California. The corresponding full symbols show data gathered by Trifunac (1993a,b) from various published seismological estimates. The thick lines represent L_R and W_R as defined in Eq. (5) and used in this paper.

The next important part of this analysis is the choice of scaling law for the permanent displacement across the fault. We considered adopting one of the published models, in particular, those of Wells and Coppersmith (1994), and the models for $d_{\max}$ of Lee et al. (1995), where $d_{\max}$ is the peak of strong motion ground displacement. The former present models that are linear fits through worldwide data for the logarithm of surface displacement versus earthquake magnitude, separately for different types of faulting, and also for all types of faulting, valid within the range of the data. For example, for the case of "all" types of faulting (for which the regression is most stable due to the larger number of data points) they use data from 148 events, and their model is valid for magnitudes between 5.6 and 8.1. The standard deviation of the logarithm of the displacement for this regression is 0.36, or a factor of 2.3, which is comparable to the scatter of the scaling laws for prediction of amplitudes of ground shaking. The models for $d_{\max}$ of Lee et al. (1995) predict peak ground displacement as a function of earthquake magnitude, distance from the source, propagation type characteristics, and various combinations of geologic site and local soil conditions. Their models were derived by multi-step regression analysis of strong motion data of peak ground displacement (computed from recorded accelerograms, after correction for the reduction due to baseline correction and high-pass filtering), from about 2,000 three-component accelergrams recorded in the Western U.S., in such a way that *on the fault* (at zero epicentral distance) they are consistent with fault dislocation data. Based on extrapolations using physical source models, their models are valid for all magnitudes, and predict decay with distance near the source consistent with a theoretical model of radiation

from a dislocation. Further, these models are also consistent with the long period asymptote of the frequency dependent attenuation models of Lee and Trifunac (1995a,b) of ground motion in the near field. The scatter of their model is such that the standard deviation of $\log_{10} d_{max}$ is 0.38, or a factor of 2.4. We opted for one of the models of Lee et al. (1995) because of its consistency with ground shaking hazard models, which is important for structures sensitive both to ground shaking and to static displacements. As the uncertainty in the predictions remains relatively large (grater than a factor of 2), for meaningful comparison and balanced estimates of the consequences upon a structure, it is essential that the scaling laws are consistent.

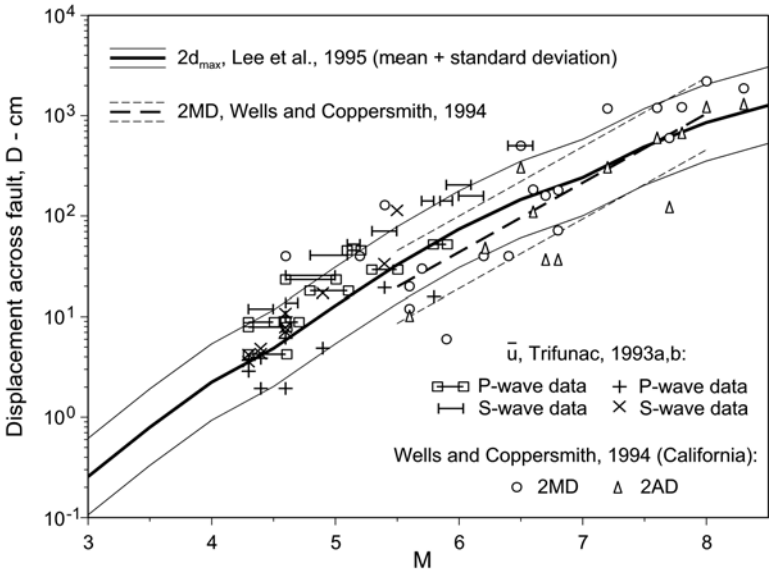

Fig. 6 Data and scaling laws for D for earthquakes in California.

We assume symmetric rupture, in which case the displacement at the ground surface across the fault, $D=2d_{max}$. While the displacement along the trace of the fault varies, and may even be discontinuous, we assume that the scaling law predicts the *average* over the length of the rupture, and that the variability is captured by the scatter of the scaling law for d_{max}. In particular, we adopted the Mag + site + soil + % rock path model for d_{max} of Lee et al. (1995), at epicentral distance R = 0 km, and for hypocentral depth $H_R = 0.5\, W_R \sin\delta$ (see Fig. 4). Furthermore we adopt the following path and site conditions: $r = 1$ (entire travel path is through rock), s = 2 ("rock" geologic site condition) and s_L = 0 ("rock" local soil condition). Lee et al. (1995) also analyzed the distribution of the residuals of $\log_{10} d_{max}$, and showed that normal distribution with mean -0.0090 and the standard deviation 0.3975 is reasonably close to the actual one. Hence, D can be modeled as lognormal random variable, such that $\log_{10} D$ has the following representation of its mean

$$\mu = M - 2.247\log_{10}\left[\Delta\left(M, R=0, H_R = 0.5\, W_R \sin\delta, S, S_0\right)/L_R\right] + 0.649M$$
$$+0.0518 * 2 - 0.341c - 2.985 - 0.137M^2 - 0.0306 + \log_{10} 2 - 0.0090 \qquad (6)$$

and standard deviation σ = 0.3975, where D is in cm, M—earthquake magnitude, Δ—(in km) "representative" source to station distance, $c = 0$ for horizontal, and $c = 1$ for vertical motions. The "representative" source to station distance, proposed by Gusev (1983), depends on physical distance and on the size of the rupture, $\Delta = S\left(\ln\dfrac{R^2 + H_R{}^2 + S^2}{R^2 + H_R{}^2 + S_0^2}\right)^{-1/2}$, where S—source dimension, and S_0—source coherence radius (both functions of magnitude), and is never zero, even for a point on the fault.

Fig. 6 shows $D=2d_{max}$ versus magnitude, as predicted by the model (the thick lines), against the data for average dislocation, $\bar{u}$, gathered by Trifunac (1993a,b), and the data for average (AD) and maximum (MD) displacement gathered by Wells and Coppersmith (1994) for California earthquakes. It can be seen that the model is in good agreement with the data. This figure also

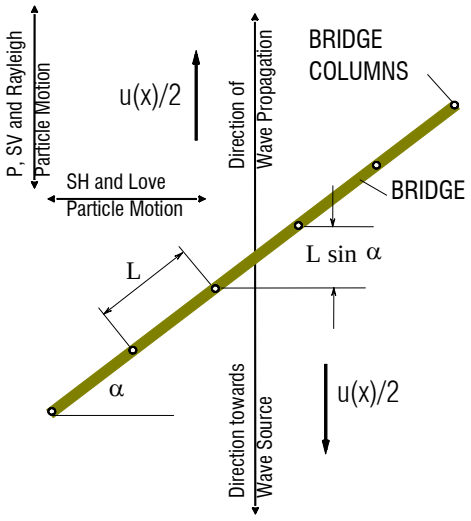

Fig. 7(a) Straight continuous bridge crossing narrow fault zone

shows the regression model of Wells and Coppersmith (the weaker lines) for average displacement for "all" types of faulting.

3. Analysis of the Combined Effects – *Continuous Girder Case*

Combination rules for estimation of the total differential displacement of the columns of a bridge will depend on the structural system and on its geometric relationship to the earthquake fault, and therefore must be formulated specifically for each structure. In the following we present an example for a continuous, straight, multi-span bridge girder, assumed to be stiff (rigid) in the horizontal plane, and supported by columns at equal spacing L. The angle between the bridge girder and the fault is determined by the specific design, but from the point of view of this analysis can be arbitrary. The surface expression of the fault can be a narrow straight line (Fig. 7(a)), or a fault zone with width G (Fig. 7(b)). For simplicity of this example it is assumed that the fault motion is pure right-lateral strike-slip. Within the fault

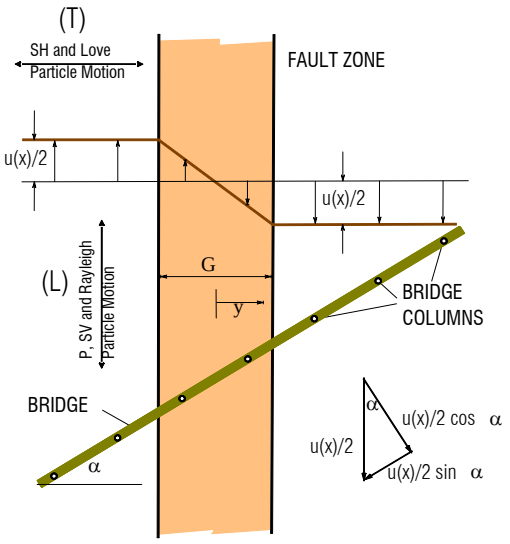

Fig. 7(b) Straight continuous bridge crossing a broad fault zone.

zone we assume that $u(x)/2$ can be approximated by $(u(x)/G)\,y$. For carefully mapped fault zones the motion within the fault zone can be modeled in more detail on a site-specific basis. We further assume that the variation of dislocations along the fault, $u(x)$, can be approximated by a parabola, with x oriented along the fault (see Fig. 4b), and with the maximum dislocation in the middle of the fault, $u_{\max} = 3D/2$ (see insert in Fig. 8), at $x = L_R/2$. We assume that the overall length of the bridge is small, relative to the fault dimensions, and therefore neglect the attenuation of permanent displacements away from the fault. All of the above assumptions can be modified, based on the

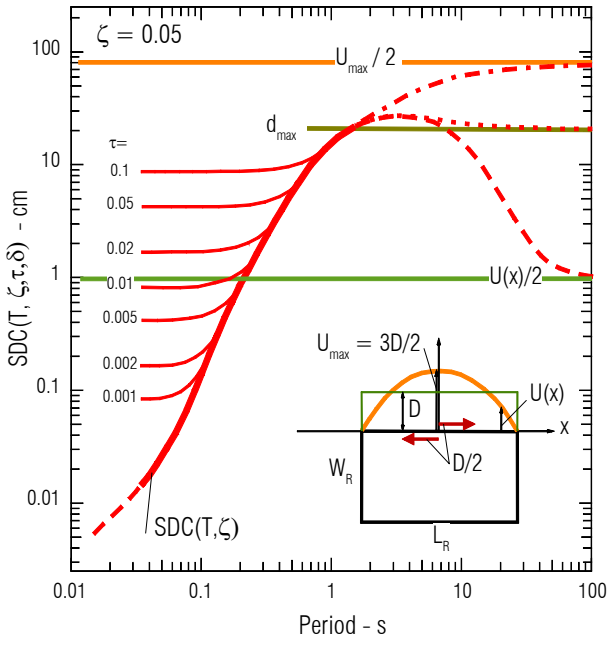

Fig. 8 Contributions to Relative Displacement Spectrum SDC: (a) inertial forces (wide solid and dashed lines, (b) differential motions (for $0.001 < \tau < 0.1$), and (c) fault slip $u(x)/2$.

detailed analysis of the bridge, its kinematic constraints, of site geometry, geological interpretation of the expected fault motion, expected seismic activity on the fault and preferred method for combining the loads. However, when analyzing relative displacements and relative rotations of structural components for bridges not comprised of continuous girders on the segments crossing the fault, each site will have to be examined on an individual basis. The following example illustrates the deterministic, worst-case scenario, and leaves presentation of the associated probabilistic method of combining different displacements for a future study.

In Fig. 8 the solid continuous line, labeled $SD(T,\varsigma)$ represents the standard relative displacement spectrum. It can be evaluated by considering one of the classical examples reviewed in Fig. 1, or in terms of modern direct empirical scaling equations (e.g., Lee, 2002). Continuation of this curve into the long period range, say beyond 1s periods, will asymptotically approach $u_{\max}/2$, or $u(x)/2$ depending where the bridge site is relative to the fault length. In either case the very long period amplitudes of $SD(T,\varsigma)$ will be determined by the permanent ground displacement

at the location of the structure. During earthquake the largest dynamic displacement pulse with amplitude $d_{\max}$ may also contribute to intermediate and long period ground motions and thus to the response of the structure.

In this example we include only those earthquakes that occur on the fault intersecting the bridge. The arrival of energy along the fault surface will produce predominantly P, SV and Rayleigh wave motions with displacement amplitudes in the direction along the fault surface (L). The SH and Love waves will produce the motions with displacements perpendicular to the fault surface (T). Assuming simultaneous action of dynamic and pseudo static effects from the differential motions alone, the resultant SDC amplitudes will be

$$SDC = \left\{ \begin{matrix} u^2_{\max_L} + \left(v_{\max_L} \sin^2\alpha + v_{\max_T} \sin\alpha\cos\alpha \right)^2 \tau^2 + \\ u^2_{\max_T} + 2\left(v_{\max_T} \sin^2\alpha + v_{\max_L} \sin\alpha\cos\alpha \right)^2 \tau^2 \end{matrix} \right\}^{1/2} . \quad (7)$$

Assuming $T_{IP} \sim T_{OP} \sim T$, $\varsigma_{IP} \sim \varsigma_{OP} \sim \varsigma$, $u_{\max_L} \sim u_{\max_T} \sim SD(T,\zeta)$, and $v_{\max_L} \sim v_{\max_T} \sim v_{\max}$, we obtain

$$SDC = \left\{ 2(SD)^2 + 3v^2_{\max}\tau^2 \left(\sin^2\alpha + \sin\alpha\cos\alpha \right)^2 \right\}^{1/2} \quad (8)$$

Adding the contribution of the relative fault motion, $u(x)/2$, then gives the final answer

$$SDC = \left\{ 2(SD)^2 + 3v^2_{\max}\tau^2 \left(\sin^2\alpha + \sin\alpha\cos\alpha \right)^2 + u^2(x)/4 \right\}^{1/2} . \quad (9)$$

The dislocation rise time (Trifunac and Novikova, 1995) and the multiplicity of the source (Trifunac and Brune, 1970) could be longer than the duration of strong motion. Hence, to be conservative, we assume the worst case scenario, that the time windows of strong motion shaking (coincident with the time window when differential motions are the largest), and of the fault displacement rise time overlap. In Eq. (9), the term $\left(\sin^2\alpha + \sin\alpha\cos\alpha \right)^2$ then monotonically grows from zero at $\alpha = 0^0$ to maximum equal to 1.4 near $\alpha = 70^0$, and then decreases to one at $\alpha = 90^0$. Thus, the contribution of the differential wave motions to SDC is zero when the bridge is perpendicular to the fault ($\alpha = 0^0$), and near maximum when the bridge is almost parallel to the fault ($\alpha = 90^0$). Inhomogeneities of the rocks in the fault zone and the associated scattering of the waves will smear these simple trends, resulting in arrivals which could be represented by a distribution of αs, and averaging out of the differential motion effects. Comparison of the amplitudes in Figs. 3 and 6 shows that $v_{\max}\tau$ and D have comparable amplitudes when $\tau = 1$. For typical bridge structures $\tau < 0.1$ and therefore the relative contribution of differential wave motions will be small for x near $L_R/2$, and may become important only near the ends of the fault ($x = 0$ and $x = L_R$). For $x < 0$ and $x > L_R$, $u(x) = 0$, and the differential wave motion becomes the only contributing term in Eq. (9).

4. Discussion and Conclusions

The purpose of this note has been to illustrate a simple design approach and an example on how to analyze simultaneous action of inertial forces, differential motions (caused by passage of strong motion waves), and of fault displacements, all accompanying an earthquake event, on a fault crossing a structure. Based on the previous experience with elements of this type of analysis, we show how the result can be presented as a superposition, via square root of the sum of the squares (SRSS) of (1) relative spectral displacements, SD, of the single degree of freedom system for shaking above the moving fault, (2) pseudo static deformation of columns caused by propagation of seismic waves through the soil, and (3) the slip on the earthquake fault. To simplify presentation, the method of analysis is illustrated in terms of horizontal ground motions only, strike-slip fault motion, and for a stiff continuous bridge supported by equally spaced columns. This approach can be generalized to simultaneous action of horizontal and vertical motions and to other structural systems.

The results are illustrated in a deterministic framework, for the worst-case scenario, when a large earthquake occurs directly beneath the structure. In this case, the main contributions to the extreme forces in the structural columns come from the dynamic response to strong shaking, and from the pseudo-static fault displacements. During such an event, typical contributions from differential wave motions will be small (about one order of magnitude smaller). A more general

approach will be to consider the contributions of all events in the area surrounding the structure, not just of the earthquakes on the fault crossing the structure, and then to perform a hazard analysis (Todorovska et al, 2005). In that case the final result will depend on the relative size of the fault crossing the structure, the size of and distances to the active faults in the area surrounding the structure, their seismic activity, and on the nature of the expected faulting. Such generalizations will be presented in future papers.

5. References

1. Biot, M.A. (1932). Vibrations of Building During Earthquake, Chapter II in *Ph.D. Thesis No.* 259 entitled "Transient Oscillations in Elastic Systems", Aeronautics Department, Calif. Inst. of Tech., Pasadena, California.
2. Biot, M.A. (1941). A Mechanical Analyzer for the Prediction of Earthquake Stresses, *Bull. Seism. Soc. Amer*., **31**(2), 151-171.
3. Biot, M.A. (1942). Analytical and Experimental Methods in Engineering Seismology, *ASCE, Transactions*, **108**, 365-408.
4. Gusev A.A. (1983). Descriptive statistical model of earthquake source radiation and its application to an estimation of short-period strong motion, *Geophys. J. Royal Astr. Soc.* **74**(3), 787–808.
5. Housner, G.W. (1959). "Behavior of Structures During Earthquakes," *J. of Eng. Mechanics Division, ASCE*, **85**(4), 109-129.
6. Lee, V.W. (2002). "Empirical Scaling of Strong Earthquake Ground Motion-Part I: Attenuation and Scaling of Response Spectra," *Indian Society of Earthquake Technology Journal*, **39**(4), 219-254.
7. Lee V.W., Trifunac M.D. (1995a)*. Frequency dependent attenuation function and Fourier amplitude spectra of strong earthquake ground motion in California, Dept. of Civil Engineering Report No CE 95-03, University of Southern California, Los Angeles, California.
8. Lee V.W., Trifunac M.D. (1995b)*. Pseudo Relative Velocity Spectra of Strong Earthquake Ground Motion in California, Dept. of Civil Engineering Report No CE 95-04, University of Southern California, Los Angeles, California.
9. Lee V.W., Trifunac M.D., Todorovska M.I., Novikova E.I. (1995)*. Empirical equations describing attenuation of the peaks of strong ground motion, in terms of magnitude, distance, path effects and site conditions, Dept. Civil Eng. Report No. 95-02, Univ. Southern California, Los Angeles, California.
10. Newmark, N.M., Blume, J.A., and Kapur, K.K. (1973). "Seismic Design Criteria for Nuclear Power Plants," *J. of the Power Division, ASCE*, **99**, 287-303.
11. Todorovska, M.I., Trifunac, M.D. (1990). Note on Excitation of Long Structures by Ground Waves, ASCE, EMD, **116**(4), 952-964.
12. Todorovska M.I., Trifunac M.D., Lee V.W. (2005). Probabilistic Assessment of Permanent Ground Displacement Across Earthquake Faults, Proc. of Earthquake Engineering in the 21st Century to mark 40th anniversary of IZIIS - Skopje, August 28-Sptember 1, 2005, Skopje and Ohrid, Macedonia, (2005).
13. Trifunac, M.D. (1976). Preliminary Analysis of the Peaks of Strong Earthquake Ground Motion – Dependence of Peaks on Earthquake Magnitude, epicentral distance and recording site conditions, Bull. Seism. Soc. Amer. **66**(1), 189-219.
14. Trifunac, M.D. (1978). Response spectra of earthquake ground motion, ASCE, EM5, **104**, 1081-1097.
15. Trifunac M.D. (1993a)*. Broad Band Extension of Fourier Amplitude Spectra of Strong Motion Acceleration, Dept. of Civil Eng., Rep. No. CE 93-01, Univ. Southern California, Los Angeles, California.
16. Trifunac M.D. (1993b). Long period Fourier amplitude spectra of strong motion acceleration, *Soil Dynam. & Earthqu. Engng* **12**(6), 363–382.
17. Trifunac, M.D. (1997). Differential earthquake motion of building foundations, *J. Structural Eng., ASCE*, **123**(4),414-422.
18. Trifunac, M.D. (2006a). Biot Response Spectrum, *Soil Dynamics and Earthquake Eng.*, **26**(6-7), 491-500.
19. Trifunac, M.D. (2006b). Brief history of computation of earthquake response spectra, *Soil Dynamics and Earthquake Eng.*, **26**(6-7), 501-508.
20. Trifunac, M.D., Brune, J.N. (1970). Complexity of energy release during the Imperial Valley, California earthquake of 109, *Bull. Seism. Soc. Amer.*, **60**, 137-160.
21. Trifunac, M.D., Gicev, V.(2006). Response Spectra for Differential Motion Columns, Paper II: Out-of-Plane Response, *Soil Dynamics and Earthquake Engineering*, **26**(12), 1149-1160.
22. Trifunac, M.D., Novikova, E.I. (1995). Duration of Earthquake Fault Motion in California, *Earthquake Eng. and Structural Dynamics*, **24**(6), 781-799, 1995.
23. Trifunac, M.D., Todorovska, M.I. (1997). Response Spectra and Differential Motion of Columns, *Earthquake Eng. and Structural Dyn.*, **26**(2), 251-268.
24. Wells D.L., Coppersmith K.J. (1994). New empirical relationships among magnitude, rupture length, rupture width, rupture area, and surface displacement, *Bull. Sesm. Soc. Am.* **84**(4), 974-1002.

---

*Can be downloaded from
http://www.usc.edu/dept/civil_eng/Earthquake_eng/